An experimental investigation of water droplet impingement on a heated wax surface ☆

Samuel L. Manzello *, Jiann C. Yang

Building and Fire Research Laboratory, National Institute of Standards and Technology, 100 Bureau Drive, Stop 8662, Bldg 224, A361, Gaithersburg, MD 20899-8662, USA

Abstract

The impact of a distilled water droplet upon a heated wax surface was investigated experimentally using a high-speed digital camera. The droplet impact Weber number (*We*) was varied and the collision dynamics were investigated with the temperature of the wax surface varied from 20 to 75 °C. For each impact *We* number, the evolution of the liquid film diameter was measured as a function of surface temperature. At *We* = 27, the liquid film diameter was observed to recoil faster as the surface temperature of the wax was increased. At *We* = 150, as the droplet recoiled, an unstable column of fluid was observed to rise above the wax surface. The instability of the fluid column at *We* = 150 was explained using Rayleigh instability theory. At the melting point of the wax, 75 °C, the droplet impacted upon a liquid surface. Over the range of impact *We* numbers considered, the jet formed in the molten wax pool did not result in separation of droplets from the jet.
Published by Elsevier Ltd.

Keywords: Droplet impact; Heated surface

1. Introduction

Liquid droplet interaction with a surface has been studied for more than a century [1]. Fundamental understanding of droplet/surface interaction is important in agricultural applications, atmospheric sciences, criminal forensics, and fire suppression. The characteristics of the droplet/surface interactions depend upon the properties of the droplet, the impacted surface, impact velocity, geometry, and the medium (liquid, gas, dispersion) through which the droplet traverses prior to impact [2].

A crucial distinction in liquid droplet/surface interaction investigations is the type of impacted surface. In a broad sense, the target surface can be classified as either a solid or a liquid surface. The collision dynamics of the impinging droplet can be vastly different for liquid and solid surfaces [2]. The fluid mechanics of droplet collision with a solid surface has been studied under a variety of conditions [3–13]. Droplet collision with liquid surfaces has been studied in some detail as well [14–25].

The impact of a liquid droplet with a solid surface can result in the droplet spreading, splashing, or rebounding on a solid surface whereas the impact of a liquid droplet with a liquid surface can result in the droplet floating, bouncing, coalescing, and splashing on the liquid surface [2]. Most, if not all, of the droplet impact literature has considered droplet impingement on either a solid or liquid surface. In the present work, droplet/surface interaction was performed using distilled water droplets and a wax surface. A wax surface was selected since it allows the observation of droplet collision dynamics on a surface that changes its properties as the temperature is increased. For low surface temperatures, impact will occur on a solid surface. As the surface temperature is raised, the wax will soften, affording the investigation of droplet impact on a gradually yielding surface. Droplet/surface interaction on a heated wax

Nomenclature

d	instantaneous film diameter	μ	dynamic viscosity
D	initial droplet diameter	v	kinematic viscosity
Oh	Ohnesorge number, $Oh = \frac{\mu}{\sqrt{\rho D \sigma}}$	ρ	density
		σ	surface tension
Re	Reynolds number, $Re = \frac{\rho V D}{\mu}$		
t	time	*Subscripts*	
V	impact velocity	c	critical
We	Weber number, $We = \frac{\rho V^2 D}{\sigma}$	max	maximum
		w	wall
Greek symbols			
β	non-dimensional liquid film diameter		

surface is of importance to fire suppression as it may be considered a *first-step* to understand how water droplets would behave when impinging upon a burning surface that changes it properties with temperature (e.g. polymeric surface).

2. Experimental description

Fig. 1 is a schematic of the experimental setup which includes the droplet generator, target surface, heating element, and imaging system. Droplets were generated using a syringe pump programmed to dispense the liquid at a rate of 0.001 ml/s. The droplet was formed at the tip of the needle (22 gauge), and detached from the syringe under its own weight. The temperature of the impinging droplets was fixed at 20 °C. The wax, which was contained in a glass cylinder, was heated by placing the container on a copper block with two miniature car-

Fig. 1. Schematic of experimental setup including the droplet generator, target surface, heating element, and imaging system.

tridge heaters embedded within it. The temperature of the block was measured using a thermocouple embedded within the surface. The temperature was controlled to within ±1 °C using a temperature controller.

The imaging system used to capture droplet impingement dynamics has been described in detail elsewhere [10,11]. The impact velocity was measured by tracking the location of the droplet centroid 2 ms prior to impact using an image processing software. The initial droplet diameter was determined 2 ms prior to impact. The image processing software was used to threshold the droplet from the background and the diameter of the droplet was measured both in the horizontal and vertical direction. The difference in the diameter measured in the vertical and horizontal direction was at most 0.3 mm. The droplet diameter was defined as the average of the two measurements. The computer system was used to store the digital images for subsequent analysis (see Fig. 1).

A commercial paraffin wax was used for the experiments. This type of wax was observed to have a melting point of approximately 75 °C. To prepare the wax surface, pieces of solid wax were placed in a glass cylinder, 125 mm in diameter. The glass cylinder was heated on a hot plate to melt the wax. Wax pieces were added until a 10 mm pool of molten wax filled the glass cylinder. The pool of molten wax was then allowed to solidify by cooling for 8 h prior to performing droplet impingement experiments.

Experiments were also performed using the present experimental setup but replacing the impacted fluid, molten wax, with distilled water to compare and contrast the collision dynamics. Since water–water impact has been studied extensively for droplet/liquid surface interaction studies, the use of water for the impacted pool may be thought of as calibration fluid for the water–molten wax experiments. For consistency, the distilled water pool was maintained at depth of 10 mm, the same depth of the molten wax pool. The depth of the impacted liquid pool is known to influence the droplet collision dynamics [17,23].
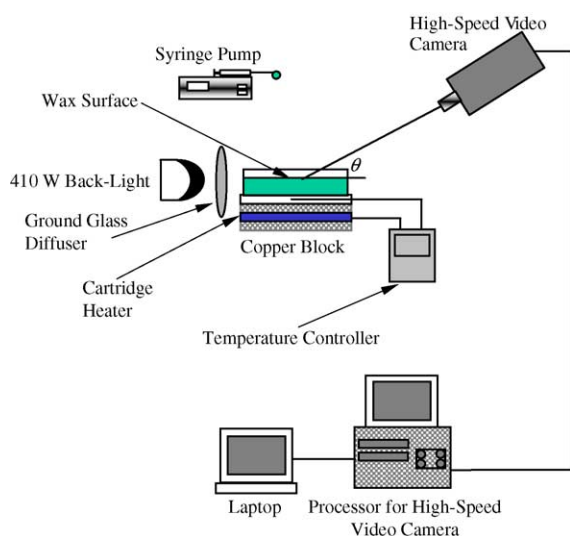
3. Results and discussion

Fig. 2 displays temporally resolved images of distilled water droplet impingement upon a wax surface at 20, 60, 70, and 75 °C for an impact Weber number of 27. The Weber number is the ratio of kinetic energy to surface energy of the droplet. Since each experiment displayed similar qualitative trends, results of three consecutive experiments were used for data analysis. The relative standard uncertainty in determining the Weber number was ±8%. At 20 °C, the droplet impacted and spread upon the surface. The liquid film then began to recoil,
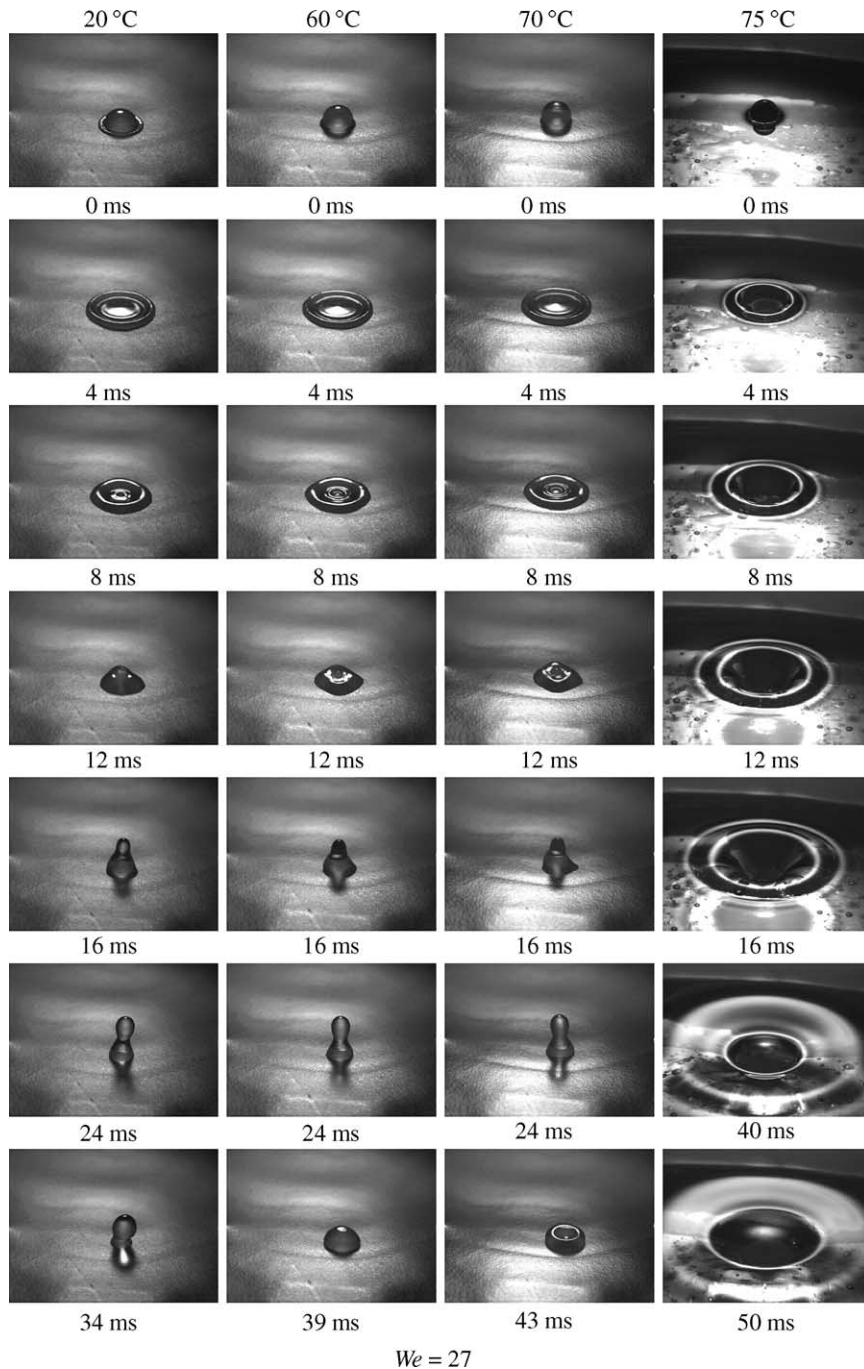

Fig. 2. Time elapsed images of distilled water droplet impingement ($We = 27$) on a wax surface at various temperatures.

and ultimately produced a near vertical column of fluid on the surface. The column of fluid ultimately collapsed upon the surface. As the surface temperature was raised, qualitatively similar collision dynamics were observed until the melting temperature was approached.

At 75 °C, the approximate melting point of the wax, dramatic differences were observed. At this temperature, a phase transition occurred in the wax. The water droplet no longer makes contact with a solid surface, rather the droplet impacted upon a molten wax surface. A crater was formed, and the crater continued to penetrate into the molten liquid until a time of ≈16 ms.

The collision dynamics are displayed in Fig. 3 for water droplet impingement upon the wax surface for an impact *We* number of 150. The *We* number was varied by increasing the height of the syringe pump from the surface. For impact at *We* = 150 with a surface temperature of 20 °C, the droplet spread over the wax surface, and rebounded. The cylindrical column of fluid became unstable and a droplet was pinched off at the tip. Qualitatively similar behavior was observed at a surface temperature of 60 °C. At a surface temperature of 70 °C and *We* = 150, the dynamics were similar to *We* = 27, namely the column of fluid formed after rebound did not breakup.

For droplet impingement upon the molten wax surface (75 °C) at *We* = 150, a more pronounced crater was observed after impact. The depth of the crater penetrated the liquid surface, and a jet was observed to emanate from the crater. The crater and jet dynamics were affected as the impact *We* number was increased (cf. Figs. 2 and 3).

Clearly, the column of fluid formed after the droplet rebounded was unstable at *We* = 150. A vast amount of literature is available regarding liquid jet breakup due to instability [26,27]. These studies have focused on the breakup of a liquid jet comprised of a single fluid emanating from a nozzle into a quiescent gas. These analyses were extrapolated to the present experiments by assuming that the column of fluid that rises above the wax surface is similar to a jet emanating from a nozzle. Thus, the term jet and liquid column of fluid on the wax surface will be used interchangeably.

Reitz and Bracco [28] have delineated jet breakup into four different regimes, Rayleigh regime, wind-induced regime, second wind regime, and the atomization regime. The type of breakup observed in the present experiments is not characteristic of very high jet velocities (i.e. second wind and atomization regime). Rather, it is assumed that liquid jet breakup occurred within the Rayleigh breakup regime. Within the Rayleigh breakup regime, the size of the droplets pinched off from the jet are on the order, or larger, than the jet diameter. Such behavior was observed in the present experiments. For the Rayleigh breakup regime, the breakup length of the

jet scales linearly with the jet velocity [27], assuming a constant nozzle diameter. For the present analysis, the diameter of the jet was assumed to be the base of the liquid column. The base of the liquid column was measured as function of impact *We* number and did not vary significantly. Accordingly, the nozzle diameter was essentially constant in these experiments. Thus, a jet with a given velocity must reach a certain length before droplets can be pinched off from the jet. The velocity of the jet issuing from the wax surface was estimated from the images of the collision dynamics. At 20, 40, and 60 °C, the velocity of the jet rising from the wax surface at *We* = 150 pool is considerably higher than the velocity of the jet rising from the wax surface at *We* = 27. For example, for *We* = 27 and *We* = 150 at 20 °C, the jet velocity was estimated to be 0.25 ± 0.027 and 0.35 ± 0.04 m/s, respectively (mean ± standard deviation). The lower velocity of the water jet at *We* = 27 suggests that the jet velocity is too low to reach the necessary breakup length. This increase in jet velocity may be the reason why the column of fluid is able to separate at *We* = 150.

The increase in jet velocity at high *We* number is due to the fact that the droplet spreads more at high *We* number [29]. When the liquid film spreads further, it is able to recoil faster, due to the larger driving force between the maximum liquid film diameter and the equilibrium value.

At 70 °C, however, the column of fluid *did not* become unstable at *We* = 150. The reason for this is due to differences in surface roughness. The wax began to make a phase transition from solid to liquid at 70 °C. Closer inspection of the surface at 70 °C revealed small bumps on the surface. At 70 °C, the enhanced roughness of the surface affected the ability of the liquid film to regroup, and form a liquid column (jet). This resulted in a lower jet velocity, in effect precluding breakup of the jet at 70 °C.

Disturbances were observed along the periphery of the liquid film at *We* = 150. Such disturbances were not observed at *We* = 27. As the droplet impacts the surface, the liquid film formed spreads radially outward and the fluid experiences a large deceleration due to retardation by viscous forces. Allen [30] believed this decelerating interface results in a Rayleigh–Taylor instability, namely an instability that exists when an interface of two different fluids is accelerated towards the fluid of higher density [31]. The Rayleigh–Taylor instability results in an interfacial wave along the edge of the expanding liquid film.

Thoroddsen and Sakakibara [32] investigated the disturbances along the periphery of the spreading liquid film as well. In their study, multiple flash-photography was used to image the changes that evolve as the liquid film expands. Based on experimental observations, they believed that the disturbances are the result of a
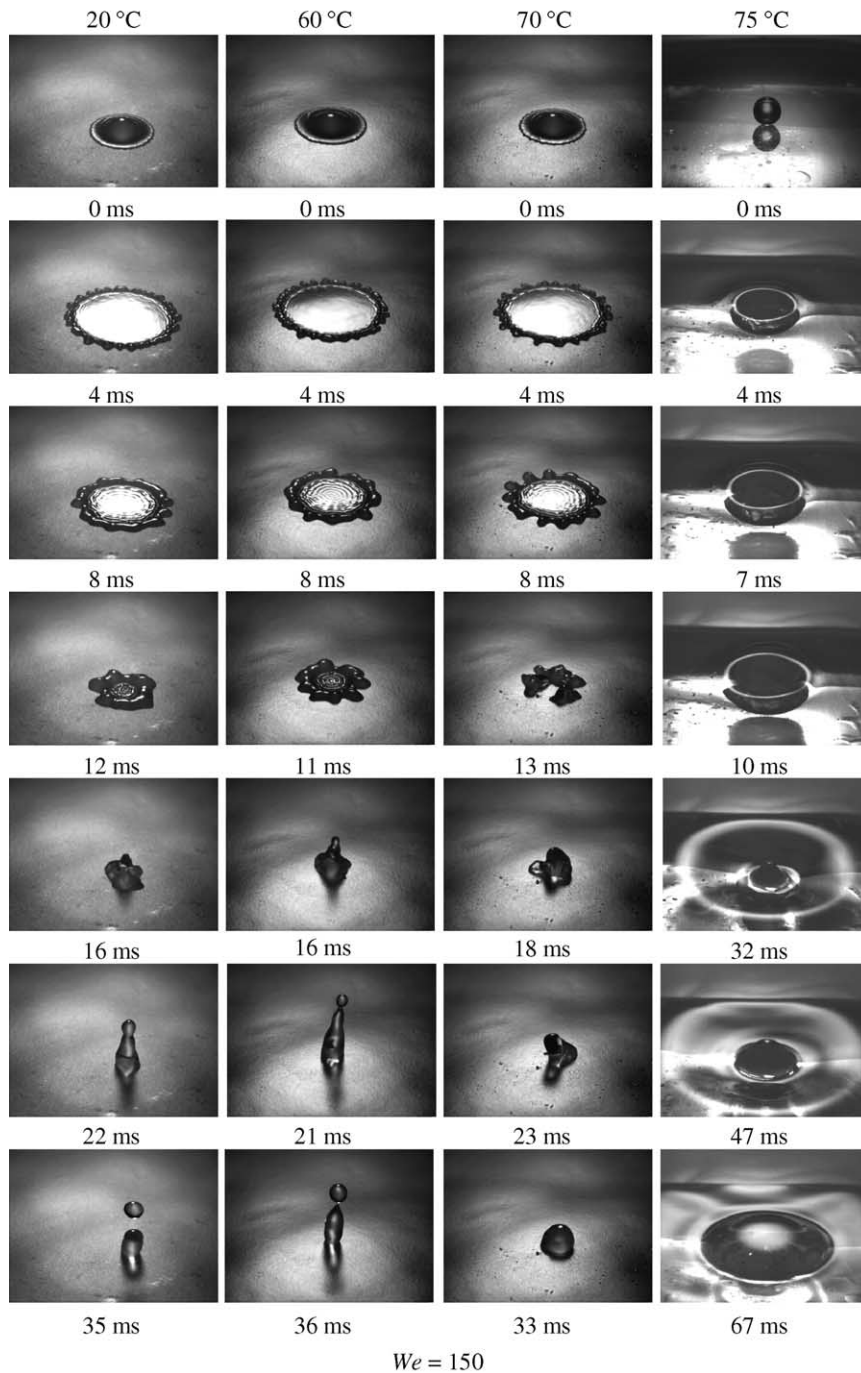
Fig. 3. Time elapsed images of distilled water droplet impingement ($We = 150$) on heated wax surface at various temperatures.

Rayleigh–Taylor instability, but the source of the instability is different than the one purported by Allen [30]. Namely, the instability is the result of a fluid ring that decelerates before making contact with the bottom of the solid surface. Although debate exists in the liter-ature about the exact cause of the Rayleigh–Taylor instability, the present experiments demonstrate that these instabilities exist for droplet impingement on a wax surface at $We = 150$, and do not seem to be influenced markedly by changes in surface temperature.

The evolution of the non-dimensional liquid film diameter with time was measured as a function of temperature for $We = 27$ and $We = 150$, and is displayed in Fig. 4. Such measurement is important in fire suppression as it quantifies the portion of surface undergoing cooling. The non-dimensional liquid film diameter was defined as, $\beta = d/D$. The non-dimensional liquid film diameter was obtained from the average of three measurements at each temperature, with the error bars representing the standard deviation. For low impact We number, the liquid film diameter was measured up to time it reached its equilibrium value (i.e. shape of sessile droplet on wax surface). For impact at $We = 150$, the liquid film diameter was measured up to time the droplet detached from the column of fluid. Due to the phase transition that was observed to occur, the non-dimensional liquid film diameter was not measured at 70 °C for $We = 27$ and $We = 150$.

Three distinct regimes were observed for impact at $We = 27$. After droplet impact, the liquid film expanded to a maximum value. The liquid film began to recoil, and reached a minimum value. The minimum value corresponded to the time of the maximum extension of the liquid column of fluid on the surface. With the collapse of the liquid column, the liquid film once again increased in magnitude, and then recoiled again, and reached the final equilibrium value.

These observations were in qualitative agreement with previous investigations on wax surfaces at 20 °C [9,33,34]. Ford and Furmidge [33] considered water droplet impact at 20 °C on a beeswax surface. A con-

tinuous stream of droplets was generated using a vibrating blade generator, and the droplets fell onto a slowly rotating surface containing beeswax. The collision dynamics were photographed using a stroboscopic lamp. They observed three distinct stages in the evolution of film diameter, initial spreading, retraction, and secondary spreading. Fukai et al. [34] performed water droplet impact experiments on a commercial wax surface, and measured the non-dimensional liquid film diameter at 20 °C. They reported qualitatively similar behavior to Ford and Furmidge [33]. The influence of temperature on the collision dynamics was not investigated.

At impact $We = 150$, the non-dimensional liquid film diameter expanded to a maximum, and then recoiled (see Fig. 4). However, ≈ 30 ms, the liquid column became unstable, and a droplet was pinched off from the surface, precluding further measurement of the liquid film diameter. At $We = 150$, the liquid film diameter was larger than that at $We = 27$.

Several correlations are available to calculate the maximum non-dimensional spread diameter within the film evaporation regime. In a recent review by Healy et al. [35], seven correlations were tested using a variety of experimental data available in the literature. It was reported that the Kurabayashi–Yang correlation provided the best agreement between the prediction and measured β_{max} for data in the film evaporation regime. Manzello and Yang [11] also reported good agreement for water droplet impact on polished stainless steel surfaces within the film evaporation regime using the Kurabayashi–Yang correlation. The Kurabayashi–Yang correlation, provided in Yang [36], is given as:

$$\frac{We}{2} = \frac{3}{2}(\beta_{max})^2 \left[1 + \frac{3We}{Re}\left((\beta_{max})^2 \mathrm{Ln}(\beta_{max}) \right. \right.$$
$$\left. \left. - \frac{(\beta_{max})^2 - 1}{2} \right) \left(\frac{\mu}{\mu_{wall}} \right)^{0.14} - 6 \right] \qquad (1)$$

where $\beta_{max} = d_{max}/D$. The Kurabayashi–Yang equation was obtained based upon an energy balance between the initial condition, and the final, fully spread condition, and is valid up to the saturation temperature of pure water. The comparison between the measured non-dimensional liquid film diameter and the predicted values at 20 °C are displayed in Table 1. Overall, the
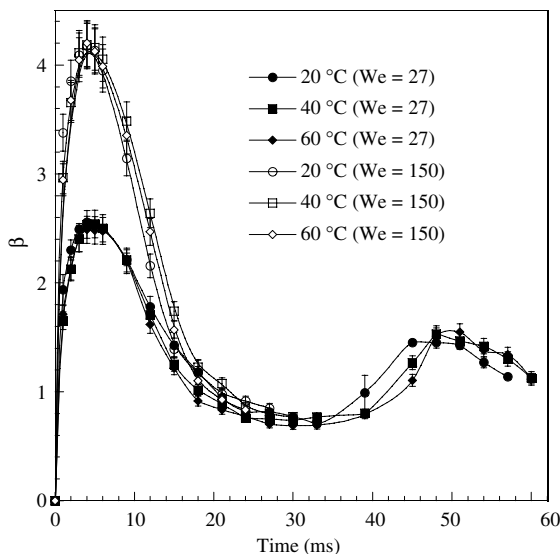

Fig. 4. Measured non-dimensional liquid film diameter as a function of time for various temperatures for droplet impingement at $We = 27$ and $We = 150$.

Table 1
Comparison of measured and predicted maximum non-dimensional liquid film diameter

We	$\beta_{max,measured}$	$\beta_{max,predicted}$
27	2.5	3.2
150	4.0	4.5

correlation provided better agreement at higher impact *We* number.

To investigate the influence of surface temperature on droplet recoil, the recoil speed was measured as a function of temperature for *We* = 27, and is plotted in Fig. 5. The recoil speed was defined as the average velocity of the liquid film diameter from its maximum extension to the time the liquid film diameter passed through the equilibrium value [29]. Cleary, the recoil speed increased as the surface temperature was increased. The recoil speed was not measured at *We* = 150 since the equilibrium value of the droplet could not be determined due to jet breakup (i.e. two droplets appeared on the surface after the collision dynamics ended).

Kim and Chun [29] suggest that the initial spreading of the droplet on the surface is governed by the impact *We* number, whereas the Ohnesorge number and equilibrium contact angle govern the recoil stage. The Ohnesorge (*Oh*) number is the ratio of the viscous force to surface tension force and is a measure of the resisting force during recoil. They reported that for fixed impact energy (fixed *We* number), the initial spreading processes were almost identical, yet the recoiling was dependent on the *Oh* number. In the present experiments, at *We* = 27, the maximum value of the non-dimensional liquid film diameter was nearly identical with temperature, yet the recoil speed increased with temperature. To evaluate the effective *Oh* number, the liquid properties are estimated at a film temperature, $(T_s + T_l)/2$, where T_s and T_l are the surface and liquid droplet temperature, respectively. For water, the dynamic viscosity, density, and surface tension decrease with temperature. It may be expected that
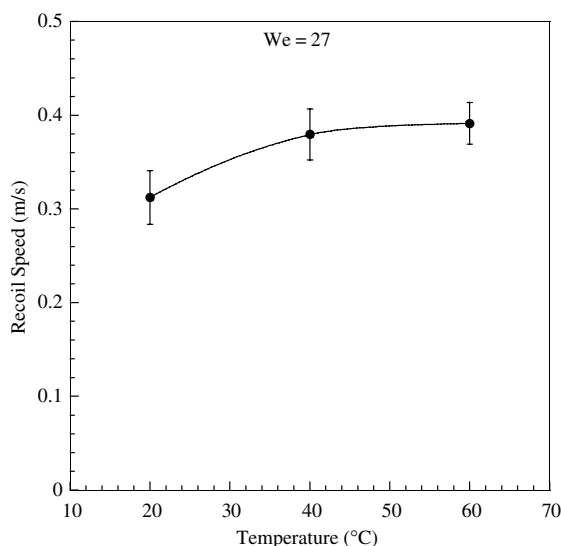
as temperature is increased, the *Oh* number would decrease. However, the experiments revealed the droplet impact process was completed within ≈60 ms. It is not expected that the droplet temperature will rise significantly within this time frame. The observed differences in recoil speed are not likely due to changes in the effective *Oh* alone. The equilibrium contact angle was also found to play a role in droplet recoil [29]. The present experiments demonstrate that the equilibrium contact angle does not vary widely with temperature.

The differences in droplet recoil speed at *We* = 27 are believed to be caused by changes in surface roughness as the temperature of the wax was increased. The measurement of the liquid film diameter supports this supposition. At *We* = 27, as the surface temperature was increased, the evolution of the liquid film diameter was nearly identical in the early stages of impact, i.e. up to the maximum liquid film diameter. Only during droplet recoil were differences observed. Although the recoil speed was not measured at *We* = 150 since the equilibrium value of the droplet could not be determined due to jet breakup, images of droplet impact dynamics show that the recoil process was affected by wax surface properties.

These experiments revealed some salient features of droplet impact dynamics on a wax surface. As the droplet impacts the surface, the kinetic energy of the impinging droplet is used to do work against viscous forces and spread the droplet onto the surface. After the droplet is completely spread out, surface tension forces do work against viscous forces to restore the liquid film to the shape of a sessile droplet upon the surface. The time scale of the recoil process is 3–4 times longer than the initial spreading process. It was observed that the droplet recoil process is indeed more susceptible to small changes in surface properties. The reason that the recoil speed did not change much above 40 °C is most likely due to the physical properties of wax itself. Prior to reaching the melting point, paraffin wax is known to reach a transition temperature where the wax begins to soften and take on a glassy appearance. Measurements of recoil speed at *We* = 27 suggest that as the transition temperature is reached, the surface of the wax becomes smoother which allows the droplet to recoil faster. Eventually the melting temperature is approached and the surface of the wax starts to deteriorate, greatly enhancing the roughness of the surface.

At 75 °C, the melting point of the wax, the water droplets no longer impacted a solid surface. Rather, the wax has completely melted and the droplet impacted a liquid surface. At the melting point of the wax, the viscosity of the wax decreased enough to support a viscous flow within the pool due to the energy exchange with the impinging droplet. This was evidenced by the observation of splashing. Splashing, defined as the appearance of a jet rising from the liquid free surface, was observed

Fig. 5. Measured recoil speed as a function of temperature for distilled water droplets at *We* = 27.

within the wax pool at $We = 150$. It is known that, for splashing, as the droplet impacts the liquid surface, a crater is formed. The crater ultimately reaches a maximum depth and fluid begins to flow radially inward to fill the crater. As fluid begins to flow into the crater, the bottom most point of the crater remains fixed. After this, a column of liquid begins to rise up from the bottom of the cavity. A jet is formed at the bottom of the crater and propelled towards the free surface as the bottom of the crater rises.

Fig. 6 displays water droplet impact into a 10 mm water pool at an impact $We = 130$. Comparing the impact of water–molten wax to water–water required matching the impact We number in addition to the pool depth. Matching the We number exactly is difficult since the We number is obtained from statistical averages of droplet diameter and impact velocity. The relative standard uncertainty in determining the We number was ±8%. Within experimental uncertainty, a We number of 130 may be considered similar to the We number of 150 for water–molten wax impact. Comparing these images with water droplet impact into the molten wax pool, differences are observed. Water droplet impact into the water pool results in a splash with a jet (defined here as the column of liquid rising from the liquid surface) breaking up at a time of 35 ms after impact. For impact with molten wax, a jet begins to rise from the pool. This jet does not breakup, as in the water pool due to differences in thermophysical properties.
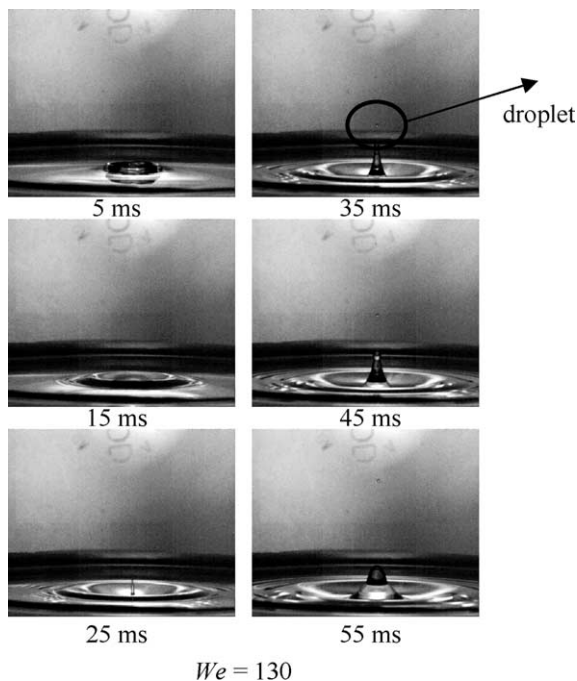

Fig. 6. Time elapsed images of distilled water–water impact ($We = 130$).

An important consideration for droplet impact into a liquid pool is the critical We number for jet breakup, We_c. If the We number of the impinging droplet exceeds the critical We number for jet breakup, We_c, droplets will separate from the jet formed within the impacted pool. These droplets will be ejected to the surroundings. The critical impact We number for jet breakup was measured for water–water impact at 10 mm and is reported to be, $We_c = 57$. The relative combined standard uncertainty in determining the critical We number was ±8%. Over the range of impact We numbers considered, the jet formed in the molten wax pool did not result in separation of droplets from the jet, therefore a critical Weber number for jet breakup could not be defined.

4. Conclusions

An experimental study was presented for distilled water droplets impacting on a heated wax surface. The droplet impact Weber number was varied and the collision dynamics were investigated with the temperature of the wax surface varied from 20 to 75 °C. For each impact We number, the evolution of the non-dimensional liquid film diameter was measured as a function of surface temperature. For impact at $We = 27$, the evolution of the non-dimensional liquid film diameter displayed three distinct regimes. Additionally, the liquid film was observed to recoil faster as the surface temperature was increased. At $We = 150$, instabilities were observed along the periphery of the spreading liquid film. The instability of the liquid column at $We = 150$ was explained using Rayleigh instability theory.

At 75 °C, the melting point of the wax, the water droplets no longer impacted a solid surface. Rather, the wax was completely melted and the droplet impacted a liquid surface. Over the range of impact We numbers considered, the jet formed in the molten wax pool did not result in separation of droplets from the jet, therefore a critical Weber number for jet breakup could not be defined.

References

[1] O. Reynolds, On the floating of drops on the surface of water depending only on the purity of the surface, Proc. Manchester Lit. Phil. Soc. 21 (1881) 1–2.
[2] M.J. Rein, Phenomena of liquid droplet impact, Fluid Dyn. Res. 12 (1993) 61–93.

[3] O.G. Engel, Waterdrop collisions with solid surfaces, J. Res. NBS 5 (1955) 281–298.

[4] S. Chandra, C.T. Avedisian, On the collision of a droplet with a solid surface, Proc. Roy. Soc. Lond. A 432 (1991) 13–41.

[5] Y.S. Ko, S.H. Chung, An experiment on the breakup of impinging droplets on a hot surface, Exp. Fluids 21 (1996) 118–123.

[6] Z. Zhao, D. Poulikakos, J. Fukai, Heat transfer and fluid dynamics during collision of a liquid droplet on a substrate2-experiments, Int. J. Heat Mass Transfer 39 (1996) 2791–2802.

[7] J.D. Bernardin, C.J. Stebbins, I. Mudawar, Mapping of impact and heat transfer regimes of water drops impinging on a polished surface, Int. J. Heat Mass Transfer 40 (1997) 247–267.

[8] B.S. Kang, D.H. Lee, On the dynamic behavior of a liquid droplet impacting upon a inclined heated surface, Exp. Fluids 29 (2000) 380–387.

[9] R. Rioboo, M. Morengo, C. Tropea, Time evolution of liquid droplet impact onto solid, dry surfaces, Exp. Fluids 33 (2002) 112–124.

[10] S.L. Manzello, J.C. Yang, An experimental study of high Weber number impact of methoxy-nanofluorobutane and n-heptane droplets on a heated solid surface, Int. J. Heat Mass Transfer 45 (2002) 3961–3971.

[11] S.L. Manzello, J.C. Yang, On the collision dynamics of a water droplet containing an additive on a heated solid surface, Proc. Roy. Soc. Lond. A 458 (2002) 2417–2444.

[12] S.L. Manzello, J.C. Yang, The effect of an alcohol resistant aqueous film forming foam (AR-AFFF) on the evaporation, boiling, and collision dynamics of a water droplet on a heated solid surface, J. Colloid Interface Sci. 256 (2002) 418–427.

[13] S. Haferl, D. Poulikakos, Experimental investigation of the transient impact fluid dynamics and solidification of a molten microdroplet pile-up, Int. J. Heat Mass Transfer 46 (2003) 535–550.

[14] J.J. Thompson, H.F. Newall, On the formation of vortex rings by drops falling into liquids, and some applied phenomena, Proc. Roy. Soc. Lond. 39 (1885) 417–436.

[15] A.M. Worthington, A Study of Splashes, Longmans, Green and Company, 1908.

[16] R.M. Schotland, Experimental results relating to the coalescence of water drops with water surfaces, Disc. Faraday Soc. 30 (1960) 72–77.

[17] W.C. Macklin, P.V. Hobbs, Subsurface phenomena and the splashing of drops on shallow layers, Science 166 (1969) 107–108.

[18] F. Rodriguez, R.J. Mesler, Some drops don't splash, J. Colloid Interface Sci. 106 (1985) 347–352.

[19] M. Hsiao, S. Lichter, L.G. Quintero, The critical Weber number for vortex and jet formation for drops impinging on a liquid pool, Phys. Fluids 31 (1988) 3560–3562.

[20] J. Shin, T.A. McMahon, The tuning of a splash, Phys. Fluids A 2 (1990) 1312–1316.

[21] M.J. Rein, The transition regime between coalescing and splashing drops, J. Fluid Mech. 306 (1996) 145–165.

[22] A.B. Wang, C.C. Chen, Splashing impact of a single drop onto very thin liquid films, Phys. Fluids 12 (2000) 2155–2158.

[23] S.L. Manzello, J.C. Yang, An experimental study of a water droplet impinging upon a liquid surface, Exp. Fluids 32 (2002) 580–589.

[24] S.L. Manzello, J.C. Yang, The influence of liquid pool temperature on the critical impact *We* number for splashing, Phys. Fluids 15 (2003) 257–260.

[25] S.L. Manzello, J.C. Yang, T.G. Cleary, On the interaction of a liquid droplet with a pool of hot cooking oil, Fire Safety J. 38 (2003) 651–659.

[26] J.W.S. Rayleigh, Further observations upon liquid jets, in continuation of those recorded in the Royal Society's Proceedings for March and May, 1879, Proc. Roy. Soc. Lond. 34 (1882) 130–145.

[27] S.P. Lin, R.D. Reitz, Drop and spray formation from a liquid jet, Annu. Rev. Fluid Mech. 30 (1998) 85–105.

[28] R.D. Reitz, F.V. Bracco, Mechanisms of breakup of round liquid jets, in: The Encyclopedia of Fluid Mechanics, Gulf, Houston, 1986.

[29] H.Y. Kim, J.H. Chun, The recoiling of liquid droplets upon collision with solid surfaces, Phys. Fluids 13 (2001) 643–659.

[30] R.F. Allen, The role of surface tension in splashing, J. Colloid Interface Sci. 51 (1975) 350–351.

[31] G. Taylor, The instability of liquid surfaces when accelerated in a direction perpendicular to their planes, Proc. Roy. Soc. Lond. A 201 (1950) 192–196.

[32] S.T. Thoroddsen, J. Sakakibara, Evolution of the fingering pattern of an impacting drop, Phys. Fluids 10 (1998) 1359–1378.

[33] R.E. Ford, C.G.L. Furmidge, Impact and spreading of spray drops on foliar surfaces, Wetting, Soc. Chem. Ind. 25 (1967) 417–432.

[34] J. Fukai, Y. Shiba, T. Yamamoto, O. Miyatake, D. Poulikakos, C.M. Megaridis, Z. Zhao, Wetting effects on the spreading of a liquid droplet colliding with a flat surface-experiment and modeling, Phys. Fluids 7 (1995) 236–247.

[35] W.M. Healy, J.G. Hartley, S.I. Abdel-Khalik, Comparison between theoretical models and experimental data for the spreading of liquid droplets impacting on a solid surface, Int. J. Heat Mass Transfer 39 (2001) 3079–3082.

[36] W.J. Yang, Theory on vaporization and combustion of liquid drops of pure substances and binary mixtures on heated surfaces, Technical Report 535, Institute of Space and Aeronautical Science, University of Tokyo, 1975.